

Noise and photoconductive gain in InAs quantum-dot infrared photodetectors

Zhengmao Ye^{a)} and Joe C. Campbell

Microelectronics Research Center, University of Texas at Austin, 10,100 Burnet Road, Bldg. 160, Austin, Texas

Zhonghui Chen, Eui-Tae Kim, and Anupam Madhukar

Department of Materials Science and Physics, University of Southern California, Los Angeles, California 90089

(Received 25 February 2003; accepted 4 June 2003)

We report noise characteristics, carrier capture probability, and photoconductive gain of InAs quantum-dot infrared photodetectors with unintentionally doped active regions. At 77 K, a photoconductive gain of 750 was observed at a bias of 0.7 V. The high gain is a result of the low carrier capture probability: $p=0.0012$. © 2003 American Institute of Physics.

[DOI: 10.1063/1.1597987]

Infrared detection (mid- and long-wavelength) has been a subject of extensive research due to its key roles in commercial, defense, and space applications. HgCdTe photodetectors continue to be performance leaders for many infrared detection applications. However, materials growth issues limit the spatial uniformity and yield, which, in turn, increase the cost of HgCdTe focal plane arrays. In the past decade, quantum-well infrared photodetectors (QWIPs), which operate on intraband transitions, emerged as an alternative for infrared detection.¹ Advantages to the QWIP approach include material uniformity and the ability to design complex multilayer, high-performance structures using advanced molecular-beam epitaxy (MBE) and metalorganic chemical vapor deposition growth technologies. A drawback to QWIPs, on the other hand, is the requirement for special coupling techniques since they do not operate in the normal-incidence mode. Another promising type of infrared photodetector, which is also based on intraband transitions, is the quantum-dot infrared photodetector (QDIP). Unlike QWIPs, QDIPs are intrinsically sensitive to normal-incident infrared radiation, owing to the three-dimensional confinement of the electrons in the QDs. Furthermore, QDIPs have longer carrier lifetimes, which creates the potential for higher photoconductive gain and higher operating temperatures.²

One figure of merit that is used to evaluate the performance of infrared photodetectors is the specific detectivity D^* , which is the signal-to-noise ratio normalized to the wavelength. Recently, QDIPs with single or dual peak photoresponse at $3\sim 14\ \mu\text{m}^{3-9}$ have been reported, among which the highest D^* is $10^{10}\ \text{cmHz}^{1/2}/\text{W}$ at 77 K.³ Although theoretical calculations suggest that QDIPs should achieve higher D^* than QWIPs,¹⁰ to date, this has not been experimentally confirmed. Current values of D^* for QDIPs are at least an order of magnitude lower than that of QWIPs. Improvements in D^* for QDIPs can be achieved by increasing the responsivity or lowering the noise. In this letter, we present a study of the noise in InAs QDIPs with unintentionally doped active regions.

The InAs QDIP studied in this work belongs to the class of $n-i-n$ structure QDIPs under examination by us.^{3,5,6,9} The sample was grown on semi-insulating GaAs (001) substrates by solid-source MBE. Five layers of nominally 3.0-monolayer (ML) InAs QDs were inserted between highly Si-doped top and bottom GaAs contact layers. Thirty-monolayer GaAs cap layers were grown via migration enhanced epitaxy at $\sim 350^\circ\text{C}$ as the QD cap layers, followed by 121-ML GaAs grown at 500°C for a total of 151-ML GaAs spacer layers. The GaAs layers between the contact layers and the nearest QD layer had a thickness of 220 \sim 240 ML.

Devices were fabricated from pieces of the same as-grown sample as reported in Ref. 9 and followed standard procedure: photolithography, wet chemical etching, metal deposition and lift-off, and rapid thermal annealing. Photolithography and wet chemical etching were used to define the device mesas, each of which had a diameter of 250 μm and a height of $\sim 1.4\ \mu\text{m}$. Electron-beam deposition of AuGe/Ni/Au and lift-off were then performed to form the top and bottom contacts. This was followed by a rapid thermal anneal at 430°C for 20 s in nitrogen. In the following discussion, “positive” bias means that a positive voltage was applied to the top contact.

The QDIP exhibited a peak photoresponse at 7.2 μm (not shown), and a spectral width of $\Delta\lambda/\lambda\sim 14\%$, which is characteristic of an intraband transition within the conduction band. The dark noise current i_n was characterized with very low noise current preamplifiers and a fast Fourier transform spectrum analyzer. The sample was mounted on a cold finger inside a cryostat and surrounded with a cold shield (dark environment). Figure 1 shows the noise current density versus frequency at a bias V_b of 0.3 V, and temperatures of 77, 90, 105, and 150 K. At low frequency ($f<2$ Hz), the dominant source of the noise current appears to be $1/f$ noise, which is characterized by an approximate dependence upon the reciprocal of the frequency and the square of the current. For $f>2$ Hz, the noise current is essentially independent of frequency. This is similar to the generation-recombination (GR) noise in bulk photoconductors and QWIPs, which leads

^{a)}Electronic mail: zmye@mail.utexas.edu

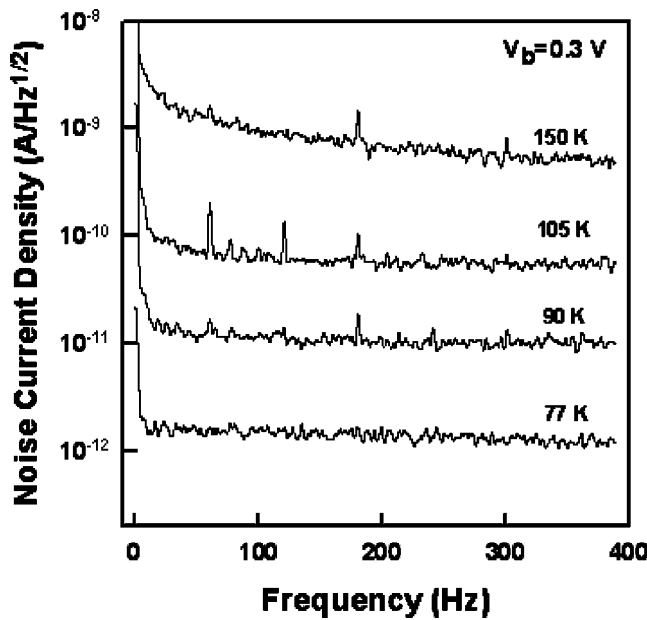


FIG. 1. Noise spectrum density vs frequency measured from 0 to 400 Hz at 0.3 V and 77, 90, 105, and 150 K.

to random fluctuations in the current density. Consequently, we hypothesize that generation and trapping processes are the dominant noise sources for QDIPs in this spectral region.

Figure 2 shows the bias dependence of the noise current at $T=77, 90, 105, 120,$ and 150 K and a measurement frequency of 140 Hz. At 77 K, the noise increases from 10^{-14} to 10^{-9} A/Hz^{1/2} as the bias increases from 0 to 0.8 V. The calculated thermal noise current I_{th} at 77 and 100 K is also shown. The thermal noise current can be expressed as

$$I_{th} = \sqrt{\frac{4kT}{R}},$$

where k is Boltzmann's constant, T is the absolute temperature, and R is the differential resistance of the device, which

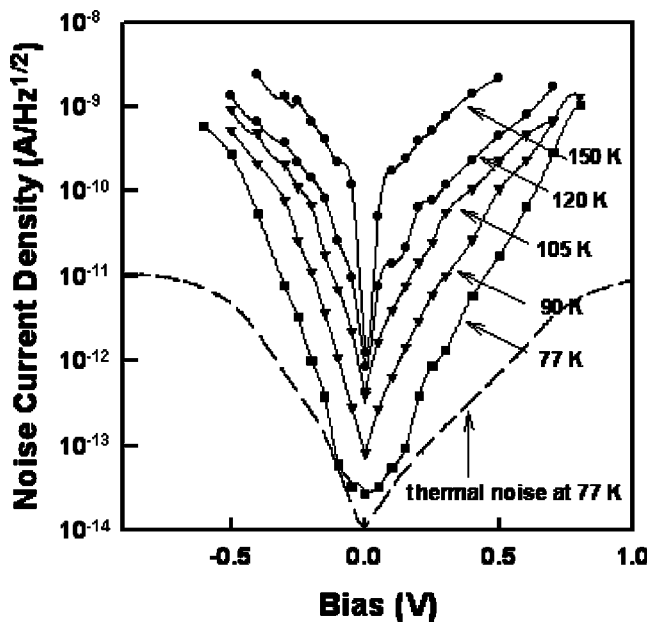


FIG. 2. Measured noise current vs bias at 77, 90, 105, 120, and 150 K. The symbols are measured data. The dashed line is calculated thermal noise current at 77 K.

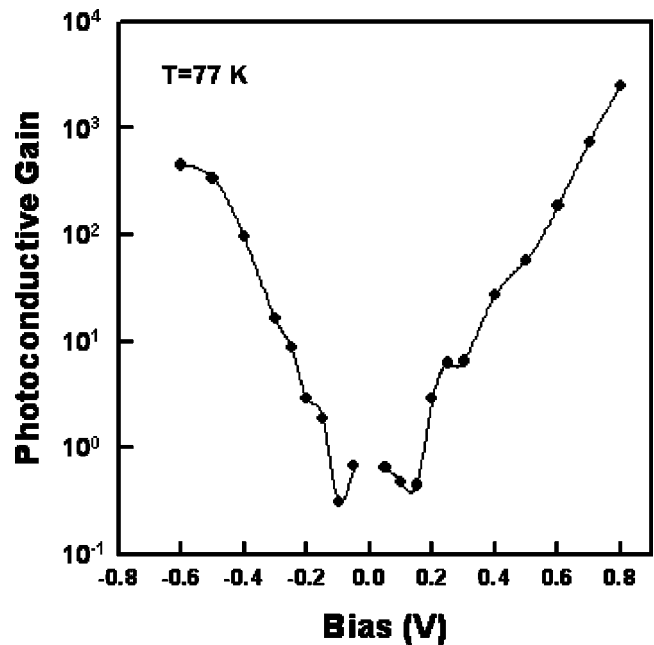


FIG. 3. Photoconductive gain vs bias at 77 K. Dots are measured data.

has been extracted from the slope of the dark current. For $V_B=0.1$ V at 77 K, the calculated thermal noise current (5.5×10^{-14} A/Hz^{1/2}) is close to the measured noise current (6×10^{-14} A/Hz^{1/2}), indicating that thermal noise is significant in the very low bias region. As the bias increases, the noise current increases much faster than thermal noise. The noise current for $|V_B| > 0.1$ V is primarily GR noise.

As a good approximation, the photoconductive gain and the noise gain are equal in a conventional photoconductor and can be expressed as

$$G = \frac{i_n^2}{4e \cdot I_d},$$

where i_n is the noise current and I_d is the dark current. The noise gain has been determined using this expression and the measured noise. Figure 3 shows the photoconductive gain at 77 K. At low bias, the gain depends weakly on voltage. With further increase in bias, the gain increases exponentially with bias again. A very large gain of 750 has been obtained at 0.7 V, corresponding to an applied electric field of 2.3 kV/cm. QWIPs typically exhibit gains in the range 0.1 to 50 for similar electric field intensities.¹¹ The higher gain of the QDIPs is the result of longer carrier lifetimes.¹²

Carrier transport in the QDIPs involves the photoexcitation of the electrons in the lower electron states in the QDs to higher energy bound states or to continuum states, transport of the excited electrons across the QDIPs, and collection or ejection of the electrons at the metal contacts. Since QDIPs have similar layer structures to those of QWIPs, the carrier transport mechanisms of the QDIPs are assumed to be similar to those of QWIPs, except that the fill factor of the QDIPs is less than unity. Therefore, compared to the gain models for QWIPs established by Liu,¹³ Beck,¹⁴ and Levine,¹⁵ Philips¹⁶ introduced a fill factor F . In this letter, we define the fill factor as the area coverage of the QDs in a QD layer. The fill factor is estimated from atomic force microscopy data. F varies from 0.40 on the first (bottom) QD layer to 0.30 on the

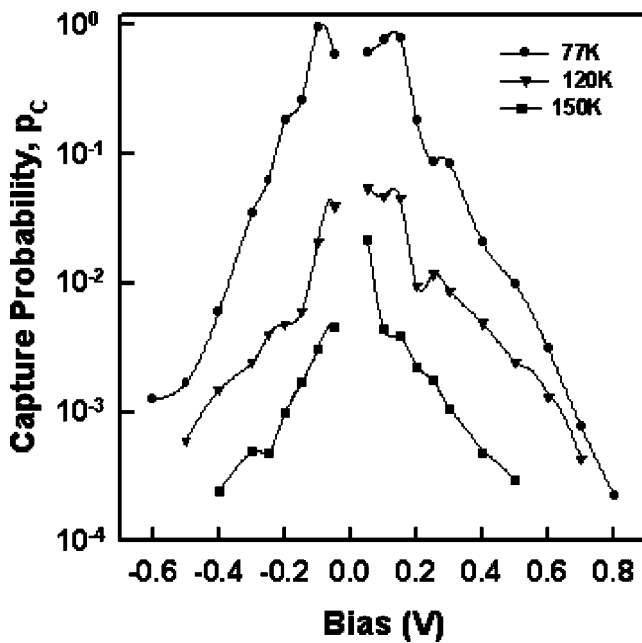


FIG. 4. Carrier capture probability versus bias at 77, 105, 120, and 150 K. Dots are measured data.

fifth (top) QD layer due to variations in the QD size and density. We combine Beck's gain expression,¹⁴ which has been experimentally verified by Schönbein,¹⁷ with the fill factor, and express the photoconductive gain as

$$g = \frac{1 - p_c/2}{FNp_c},$$

where N is number of QD layers and p_c is defined as the probability that a carrier is captured by a QD after its generation. An average value of 0.35 for F was used to calculate the capture probability. Figure 4 shows the capture probability versus bias at 77, 105, 120, and 150 K. At lower bias (-0.1 V), the capture probability is near unity. With increase in negative bias, the capture probability decreases rapidly, which results in a rapid increase in the photoconductive gain. At -0.6 V, $p = 0.0012$. Compared to conventional AlGaAs–GaAs QWIPs in which p_c is typically $\cong 0.1$, the QDIP demonstrates a gain that is several orders of magnitude larger than the QWIPs.¹⁸ With an increase in temperature, the carrier capture probability decreases rapidly. The reason is that the electron states in the QDs are most likely filled with electrons at high temperature due to the higher dark current.

The approximation that the photoconductive gain is equal to the noise gain is valid when the capture probability in Liu's¹³ and Levine's models¹⁵ is small; that is, $p_c \ll 1$. Choi examined the relationship between photoconductive gain and noise gain for QWIPs.¹⁹ His formulation is parameterized in terms of the ratio F of the noise gain g_i , to the photoconductive gain g_e ; that is, $F = g_i/g_e$. His analysis

shows that the ratio depends on t_w/t_p , where t_w and t_p are the transit times across one well and one period, respectively. For small capture probability ($p_c < 0.2$), the value of F is greater than 0.9 and relatively independent of t_w/t_p . The capture probability p_c can be calculated from noise gain and is independent of F . We have determined from the noise measurements that $p_c < 0.2$ for all bias values in the range 120 to 150 K, and for bias $|V_b| > 0.2$ V at 77 K. For the regime $|V_b| \leq 0.2$ V at 77 K, we observe that the difference between g_e and $g_i [= (1-F)g_e]$, is small for the entire range of p_c as a result of the fact that g_e is small in this region. Choi calculated g_e as a function of g_i when $t_w/t_p = 0$; that is, the case for which the largest difference between g_i and g_e would be expected. For the regime where g_e is small, which is the case for our QDIPs when $|V_b| \leq 0.2$ V at 77 K, he found that the difference is only 3% for $g_e = 0.5$. Therefore, we conclude that the noise gain provides a reliable estimation of the photoconductive gain.

In summary, we have studied the noise characteristics of InAs/GaAs QDIPs. The noise current originates from the trapping processes in the quantum dots and is GR noise in the 2–400-Hz measurement range. High photoconductive gain (> 750) has been observed owing to the low carrier capture probability: $p = 0.0012$ at -0.7 V.

This work was supported by the DoD Multidisciplinary University Research Initiative (MURI) program administered by AFOSR under Grant No. F49620-98-1-0474.

- ¹A. Goldberg, S. Kennerly, J. Little, T. Shafer, C. Mears, H. Schaake, M. Winn, M. Taylor, and P. Uppal, *Opt. Eng.* **42**, 30 (2003).
- ²V. Ryzhii, *Semicond. Sci. Technol.* **11**, 759 (1996).
- ³Z. M. Ye, J. C. Campbell, Z. H. Chen, E. T. Kim, and A. Madhukar, *Quantum Electron.* **38**, 1234 (2002).
- ⁴A. D. Stiff-Roberts, S. Chakrabarti, S. Pradhan, B. Kochman, and P. Bhattacharya, *Appl. Phys. Lett.* **80**, 3265 (2002).
- ⁵Z. M. Ye, J. C. Campbell, Z. H. Chen, E. T. Kim, and A. Madhukar, *J. Appl. Phys.* **92**, 7463 (2002).
- ⁶Z. M. Ye, J. C. Campbell, Z. H. Chen, E. T. Kim, and A. Madhukar, *J. Appl. Phys.* **92**, 4141 (2002).
- ⁷D. Pan, E. Towe, and S. Kennerly, *Appl. Phys. Lett.* **76**, 3301 (2000).
- ⁸D. Pan, E. Towe, and S. Kennerly, *Appl. Phys. Lett.* **75**, 2719 (1999).
- ⁹Z. H. Chen, O. Baklenov, E. T. Kim, I. Mukhametzhanov, J. Tie, A. Madhukar, Z. M. Ye, and J. C. Campbell, *J. Appl. Phys.* **89**, 4558 (2001).
- ¹⁰J. Phillips, *J. Appl. Phys.* **91**, 4590 (2002).
- ¹¹C. Jelen, S. Slivken, T. David, M. Razeghi, and G. Brown, *Quantum Electron.* **34**, 1124 (1998).
- ¹²V. Ryzhii, *J. Appl. Phys.* **89**, 5117 (2001).
- ¹³H. C. Liu, *Appl. Phys. Lett.* **61**, 2703 (1992).
- ¹⁴W. A. Beck, *Appl. Phys. Lett.* **63**, 3589 (1993).
- ¹⁵B. F. Levine, A. Zussmann, S. D. Gunapala, M. T. Asom, J. M. Kuo, and W. S. Hobson, *J. Appl. Phys.* **72**, 4429 (1992).
- ¹⁶J. Phillips, P. Bhattacharya, S. W. Kennerly, D. W. Beekman, and M. Dutta, *Quantum Electron.* **35**, 936 (1999).
- ¹⁷C. Schönbein, H. Schneider, R. Rehm, and M. Walther, *Appl. Phys. Lett.* **73**, 1251 (1998).
- ¹⁸B. F. Levine, *J. Appl. Phys.* **74**, R1 (1993).
- ¹⁹K. K. Choi, *Appl. Phys. Lett.* **65**, 1268 (1994).